Comment on "Systematics of radial and angular-momentum Regge trajectories of light nonstrange $q\bar{q}$-states"

D. V. Bugg

Queen Mary, University of London, London E1 4NS, United Kingdom

(Received 15 September 2012; published 3 June 2013)

Masjuan, Arriola, and Broniowski [Phys. Rev. D **85**, 094006 (2012)] claim that the slope of the light-quark radial trajectories is $1.35 \pm 0.04\ \mathrm{GeV}^2$, disagreeing with the Crystal Barrel value $1.143 \pm 0.013\ \mathrm{GeV}^2$. There are defects in their choice of data. When these defects are revised, results come back close to the Crystal Barrel average for the slope. A revised average value is given here.

DOI: 10.1103/PhysRevD.87.118501 PACS numbers: 14.40.−n, 12.38.−t, 12.39.Mk

I. INTRODUCTION

Masjuan, Arriola, and Broniowski (referred to later as MAB for brevity) report a new analysis of the slopes of trajectories [1,2]. They adopt a χ^2 criterion, which increases the errors assigned to resonance masses by up to a factor 20. They take

$$\chi^2 = \sum_n \left(\frac{M_n^2 - M_{n,\mathrm{exp}}^2}{\Gamma_n M_n} \right)^2, \tag{1}$$

where M_n and Γ_n are masses and widths of fitted resonances. Their rationale is that the extrapolation to poles off the real s-axis may be inaccurate by one half-width.

The essential point of disagreement with MAB is whether this assumption is justified or not. My point is that large uncertainties in the extrapolation to the pole arise only when a strong S-wave threshold opens in the immediate vicinity of the resonance. An example is $f_2(1565)$, which decays strongly to the $\omega\omega$ S-wave, opening precisely at 1565 MeV. In this case, there is a large dispersive contribution to the real part of the amplitude, as discussed below in Sec. III. Clearly one should be alert to such thresholds. However, most high mass resonances have many open channels, and such effects are small. After eliminating the special cases, there is no support for the assumption of Eq. (1) as the general case.

To illustrate the effect of the increased errors, it is sufficient to quote one example. The Particle Data Group (PDG) quotes a mass for the $a_4(2040)$ as 2001 ± 10 MeV [3]. For $a_4(2255)$, the PDG uses two measurements with masses 2237 ± 5 and 2255 ± 40 MeV. From these two states, MAB find a slope of $1.0 \pm 0.8\ \mathrm{GeV}^2$. This implies an error in the mass difference of 203 MeV. This is entirely inconsistent with the Crystal Barrel assessment of errors for the analytic continuation to the pole.

Further disagreements arise from several sources. There do exist some missing states, and that must be realized in drawing trajectories. Another point is that it is well known that $c\bar{c}$ and $b\bar{b}$ $^3S_1$ ground states are anomalously low in mass compared with a straight trajectory through J/ψ and Υ $n = 2, 3, 4$ radial states. There are indications that this is also true for $n\bar{n}$ states. A third point is that there is almost certainly a $J^{PC} = 0^{++}$ glueball in the mass range 1370–1800 MeV but no present agreement on its identification. It will certainly mix with $q\bar{q}$ states, and this mixing makes the masses of $q\bar{q}$ components uncertain.

A primary problem is that MAB do not distinguish clearly between $^3S_1$ and $^3D_1$ states. Conventional wisdom is that P-state light mesons appear at masses 1200–1300 MeV, D states at 1600–1700 MeV, and F states near 2000 MeV. However, they assign the third $^3S_1$ ω state a mass of ~1970 MeV, i.e., ~300 MeV above the $^3D_3\omega_3(1670)$ and $\rho_3(1690)$. The result is a slope for the $^3S_1$ ω trajectory ~4/3 times larger than other trajectories.

They also replace the best determinations of trajectories for $I = 0, C = +1$ mesons (where there are 10 sets of data) by poorer determinations of $I = 1$ $C = +1$ mesons, where there are no polarization data to separate $^3P_2$ and $^3F_2$ mesons, hence much larger errors for masses. They also replace the Crystal Barrel determination of the mass of the $f_3(2300)$ by including a possibly biased mass determination from data on $\bar{p}p \to \Lambda\bar{\Lambda}$. That is not a good idea, since mixing with the $s\bar{s}$ amplitude can confuse the situation.

In order to present the discrepancies with the slopes of trajectories assigned by Crystal Barrel (CB), the slopes of all trajectories are redetermined here from final CB data sets and tabulated for comparison with the slopes of MAB. The table of results makes the differences immediately apparent.

II. PROLOGUE

The Crystal Barrel has produced extensive data on formation of high mass mesons in the process $\bar{p}p \to R \to A + B$, where R stands for a resonance and there are 18 channels of all-neutral final states available. Reference [4] reviews the data and technical details. The detector covers 98% of the solid angle with caesium iodide crystals which measure all-neutral final states. Quantum numbers fall into four noninterfering families $I = 0$ or 1, $C = +1$ or -1.

For $I = 0$, $C = +1$, there are data on 6 channels: $\eta\pi^0\pi^0$, $\eta'\pi^0\pi^0$, 3η, $\pi^0\pi^0$, $\eta\eta$, and $\eta\eta'$. There are also differential cross sections and polarization data for $\bar{p}p \to \pi^+\pi^-$ from the PS172 [5] and an earlier experiment at the

CERN PS [6]. These are vital for two reasons. First, they separate $^3P_2$ and $^3F_2$ states. Second, polarization is phase sensitive and reduces errors on fitted masses and widths substantially. The improvement in mass determination from polarization data can be up to a factor 4 because of its phase sensitivity.

In the $\eta\pi\pi$ data, there are prominent $f_4(2050)$ and $f_4(2300)$ signals, easily identified from their strong angular dependence. They are determined accurately in mass and width from data at 9 beam momenta from 600 to 1940 MeV/c. These states serve as interferometers for all lower spin triplet partial waves. There is also a lucky break that two singlet states also appear prominently: an $\eta_2(2250)$ in $\eta'\pi\pi$ and $\eta(2320)$ in the 3η data in the channel $f_0(1500)\eta$. A complete set of $n\bar{n}$ states appears in two towers of resonances centred near 2000 and 2270 MeV. For $I = 1$, $C = -1$, an almost complete set of states also appears, but with poor identification of $^3S_1$ states. For $I = 1$, $C = +1$, there are actually two solutions, with one of them close to the $I = 0$, $C = +1$ solution, as one would expect for light quarks with small mass differences. For $I = 0$, $C = -1$, statistics are low for $\omega\eta$, and the $\omega\pi^0\pi^0$ data have the problem that the broad $\sigma \equiv f_0(500)$ interferes all over the Dalitz plot.

The F states lie systematically ~70 MeV above the P states, because high L states need to overcome a centrifugal barrier in order to resonate. The D states lie roughly midway; S and G states continue the sequence.

The $f_2(1525)$ is widely accepted as the $s\bar{s}$ partner of $f_2(1270)$. Production of $f_2(1525)$ in the Crystal Barrel experiment is extremely weak. It is detected at the 1%–2% level in $\bar{p}p \to \eta\eta\pi^0$ in flight [7]. The conclusion is that $\bar{p}p$ annihilation is dominantly to $n\bar{n}$ final states—hardly a surprise. This conclusion is supported and quantified by a combined analysis of data on $\bar{p}p \to \pi^+\pi^-$, $\pi^0\pi^0$, $\eta\eta$ and $\eta\eta'$ [8]. Amplitudes for decay to $\eta\eta$ and $\eta\eta'$ depend on the well-known composition of η and η' in terms of singlet and octet states and the pseudoscalar mixing angle. The observed state R is expressed as a linear composition $R = \cos\Phi|q\bar{q}> + \sin\Phi|s\bar{s}>$. The result is that $\Phi \leq 15°$, i.e., a maximum of 25% in amplitude, for all observed states with the exception of $f_0(2105)$ (which is taken as a glueball candidate but could possibly be due to unexpectedly strong mixing between closely spaced $n\bar{n}$ and $s\bar{s}$ states). The allocation MAB make between $n\bar{n}$ and $s\bar{s}$ states is in conflict with the fact that CB states are dominantly $n\bar{n}$.

The partial wave analysis of CB data is documented in Sec. 4 of Ref. [4]. This describes systematic checks, which have been made on the identification of resonances, particularly their stability as the number of fitted resonances was changed. The following sections illustrate the result and discuss individual resonances and their Argand diagrams. For $I = 0$, $C = +1$, all states have statistical significance >25 standard deviations except for the $f_2(2001)$, which is 18σ but observed clearly in four sets of data. Two states, $f_1(2310)$ and $\eta(2010)$, have rather large errors for masses. Regge trajectories are discussed in Sec. 9. For channels $\omega\pi$ and $\omega\eta$, polarizations of ω are determined by the angular dependence of decays to $\pi^+\pi^-\pi^0$ and are very revealing. The interpretation of this polarization is important and discussed in Secs. 7.1 and 8. There is one nonstandard piece of nomenclature. These polarizations are described as vector polarization P_y. Strictly, the standard nomenclature is that this should be called ReiT_{11}, where T is tensor polarization.

III. DETERMINATION OF SLOPES OF TRAJECTORIES

One should be aware in advance that states may deviate from straight trajectories because of dispersive effects on resonance masses. The strict form for the denominator of a Breit-Wigner amplitude is

$$D(s) = M^2 - s - m(s) - i\sum_j g_j^2 \rho_j, \qquad (2)$$

$$m(s) = \frac{1}{\pi} P \int_{\mathrm{sthr}}^{\infty} \sum_j \frac{g_j^2 \rho_j(s')ds'}{s' - s}. \qquad (3)$$

To make the principal value integral converge better, it is typical to make a subtraction on the resonance, although in principle this can be done at any mass; *sthr* is the s value at threshold for each channel. The g_j^2 are coupling constants to every decay channel, and $\rho_j(s')$ are the phase space for each final state, including centrifugal barriers and possible form factors. Near the thresholds of important decay channels, a change in the imaginary part of the amplitude is accompanied by a corresponding real part so as to obey analyticity. At sharp thresholds, the imaginary part of the phase space rises linearly from threshold and produces a cusp in the real part of the amplitude. This acts as an attractor [9]. The $a_0(980)$ and $f_0(980)$ are attracted to the $K\bar{K}$ S-wave threshold. Likewise, the $f_2(1565)$ is attracted to the sharp threshold for the $\omega\omega$ final state; this attraction is augmented by a broader threshold in the $\rho\rho$ channel, which has three times more events from the SU(2) relation with $\omega\omega$. The PDG mass is taken from the $\pi\pi$ channel, but the $\omega\omega$ and $\rho\rho$ channels are, respectively, a factor of 8.5 and a factor of 25 stronger than $\pi\pi$ when integrated over the available mass range, see Fig. 5(b) of Baker *et al.* [10]. In that paper, a dispersion relation was evaluated for the effect of both these channels; the pole position was determined to be 1598 ± 11(stat) ± 9(syst) MeV. This is lower than the $a_2(1700)$ of the PDG, but this is because of physics which is understood.

For CB data in flight above the $\bar{p}p$ threshold, there is a conspicuous $f_2(1270)\eta'$ signal fitted as an $I = 0$, $C = +1$ $J^{PC} = 2^{-+}$ resonance at 2267 MeV and clearly associated with the S-wave threshold effect, see Figs. 17 and 18 of

Ref. [4]. For $I = 1$, $C = +1$, there are signs of similar activity near the $a_2(1320)\eta'$ threshold, but this channel cannot be reconstructed accurately enough in the very difficult final state $\eta'\eta'\pi^0$. The S-wave structure could arise at thresholds for $a_2(1320)\omega$, $a_2(1320)\rho$, $f_2(1270)\omega$, and $f_2(1270)\rho$ but is blurred out by convolution of the large widths of a_2 and f_2 with the ρ. It would lead to structure distributed over $J^{PC} = 3^{--}$, 2^{--}, and 1^{--} but in the absence of polarization data cannot be sorted out at present. For P-wave thresholds, the imaginary part of the amplitude increases as the cube of the momentum and leads to negligible effects.

The $\bar{p}p$ and $\bar{p}n$ total cross sections follow a $1/v$ variation, where v is the relativistic velocity of the incident $\bar{p}$. The result is a strong cusp at the $\bar{p}p$ threshold in both $^1S_0$ and $^3S_1$ partial waves. This $1/v$ dependence is included into the partial wave analysis for these waves. This cusp will perturb masses of resonances near the threshold. Data from Novosibirsk on $\bar{p}p \to 6\pi$ final states have a rapid mass variation close to the $\bar{p}p$ threshold [11].

Returning to the question of observed slopes of trajectories, each set of quantum numbers will be examined one by one, fitting the expected states to observed masses and errors, but paying particular attention to cases where states are missing or strongly displaced by dispersive effects. Having done this, a grand average is taken of all slopes. As a guide, Fig. 1 shows the updated analysis of $I = 0$, $C = +1$ states.

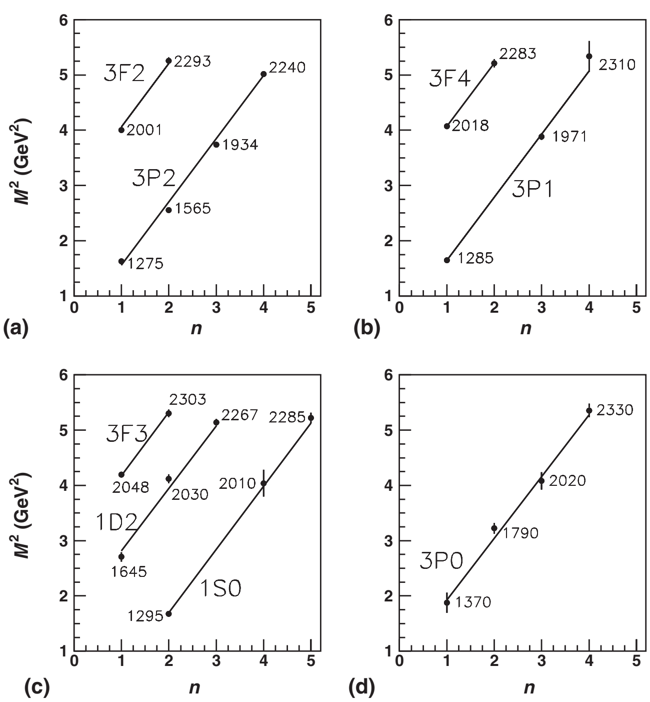

FIG. 1. Trajectories of light mesons with $I = 0$, $C = +1$ observed in Crystal Barrel data in flight, plotted against radial excitation number n; masses are marked in MeV. The average slope is adopted for all cases, so as to display discrepancies.

IV. RESULTS

Table I lists slopes for all families of light mesons in GeV^2. General comments are as follows. First, $I = 0$, $C = +1$ states are best determined because of the available polarisation data, which are very precise. For triplet states, decays are possible for orbital angular momentum $L = J + 1$ and $L = J - 1$. The ratio of coupling constants $r_J = g_{J+1}/g_{J-1}$ is tabulated in Ref. [4] but not tabulated by the Particle Data Group; it is the basic guide to whether states have $L = J + 1$ or $J - 1$.

Why should $^3F_2$ $n\bar{n}$ states decay preferentially to $\bar{p}p$ $^3F_2$? A feature of CB data is that F states decay strongly to channels with high angular momentum. The origin of this is clearly a good overlap between wave functions of initial and final states. Llanes-Estrada *et al.* point out a formal analogy with the Frank-Condon principle of molecular physics consistent with this interpretation [12].

It is immediately clear from the errors in the table that the χ^2 weighting used by MAB increases some errors by large amounts. From the agreement in many cases between CB and MAB, it is also clear that remaining discrepancies should be inspected closely. It is easiest to compare with results from MAB in their Sec. 3, taking them in the reverse order to the publication, i.e., K to A. A clear picture of disagreements then arises step by step.

The f_1 and f_3 states are considered in MAB Sec. 3K. The CB approach is to fit $f_1(1285)$, $f_1(1910)$, and $f_1(2310)$ using their errors. The first two have small errors, with the result that the fit misses the weak $f_1(2310)$ by just over one standard deviation. Neither $f_1(1420)$ nor $f_1(1510)$ is fitted well by the CB approach or that of MAB. In the CB fit, a state is expected at 1660 MeV, close to its isospin partner $a_1(1640)$. The $f_1(1510)$ is naturally assigned as the $s\bar{s}$ analogue of $f_1(1285)$; the mass difference is close to that between $f_2(1270)$ and $f_2(1525)$. Longacre proposes that $f_1(1420)$ is a molecule where an $L = 1$ pion circles a $K\bar{K}$ core [13]. For f_3, the MAB slope has an error a factor 9 larger than the CB value. Sections 3J and 3I agree well on slopes between CB and MAB for b_3, b_1, h_3, and h_1 states.

For f_3, it is clear from the slope of MAB that they use a mass well above the CB determination of the mass of $f_3(2300)$, 2303 ± 15 MeV; it seems likely that it is replaced by the value 2334 ± 25 MeV from $\bar{p}p \to \Lambda\bar{\Lambda}$ data. This is dangerous, since it may introduce mixing with $s\bar{s}$. If one takes the weighted mean of the two masses quoted by the PDG [3] for $f_3(2300)$, namely, 2311 ± 13 MeV, the slope is 1.15 ± 0.08.

Sections 3J and 3I of Ref. [1] agree between CB and MAB for b_3, b_1, h_3, and h_1 states. Section 3H considers ω states. MAB and CB agree on the ω_3 trajectory within errors. But MAB put the $\omega(1650)$ on a trajectory with an $\omega(2290)$ observed in $\bar{p}p \to \Lambda\bar{\Lambda}$. This could be an $s\bar{s}$ state or could be due to an upward shift of the $\omega(2255)$ because of the $s\bar{s}$ background. The consequence is that MAB ignore the well-known $\omega(1650)$ as a standard $^3D_1$ state.

TABLE I. Nominal resonances masses and slopes (in GeV^2) from CB and MAB analyses; comments are marked by a + in the final column and discussed in the text; a dash in column 2 indicates a missing state (or unused for reasons discussed in the text).

Family	Nominal masses (MeV)	CB slope	MAB slope	Comments
f_4	2050, 2300	1.140 ± 0.093	...	
f_3	2050, 2300	1.147 ± 0.071	1.27 ± 0.64	+
$f_2(^3F_2)$	2000, 2295	1.254 ± 0.075	...	
$f_2(^3P_2)$	1270, 1565, 1910, 2240	1.113 ± 0.025	...	+
f_1	1285, -, 1970, 2310	1.130 ± 0.064	1.19 ± 0.15	+
f_0	1370, -, -, 2330	1.24 ± 0.045	1.24 ± 0.18	+
h_3	2025, 2275	1.075 ± 0.147	1.08 ± 0.54	
h_1	1170, 1595, 1965, 2215	1.195 ± 0.059	1.20 ± 0.25	
b_3	2025, 2275	0.95 ± 0.191	1.08 ± 0.54	
b_1	1235, -, 1960, 2240	1.169 ± 0.058	1.17 ± 0.18	
ω_3	1670, 1945, 2255	1.059 ± 0.163	1.16 ± 0.26	
ω_2	1975, 2195	0.917 ± 0.160	...	
$\omega_1(^3D_1)$	1650, 1960, 2295	1.091 ± 0.068	1.27 ± 0.47	+
$\omega_1(^3S_1)$	782, 1420, 1650, -, 2.205	1.080 ± 0.029	1.50 ± 0.12	+
a_4	2040, 2255	1.000 ± 0.045	1.00 ± 0.8	
a_3	2030, 2275	1.051 ± 0.170	1.5 ± 0.11	
$a_2(^3F_2)$	2030, 2255	0.964 ± 0.128	1.00 ± 0.7	
$a_2(^3P_2)$	1320, 1700, 1950, 2175	1.000 ± 0.060	1.39 ± 0.26	+
a_1	1260, 1640, 1930, 2270	1.084 ± 0.063	1.36 ± 0.49	+
a_0	1450, 2025	0.964 ± 0.073	1.42 ± 0.26	+
π_2	1670, 2005, 2245	1.218 ± 0.062	1.21 ± 0.36	
π_0	1300, 1800?, 2070, 2360	1.29 ± 0.200	1.27 ± 0.27	
ρ_3	1690, 1990, 2265	1.094 ± 0.050	1.19 ± 0.32	+
ρ_2	1940, 2225	1.206 ± 0.085	...	
$\rho_1(^3D_1)$	1700, 2000, 2270	1.203 ± 0.052	1.08 ± 0.47	+
$\rho_1(^3S_1)$	770, 1450, -, 1900, 2150	1.365 ± 0.108	1.43 ± 0.13	+
η_2	1645, 2030, 2265	1.188 ± 0.038	1.32 ± 0.32	
η_0	1295, 2320	1.241 ± 0.030	1.33 ± 0.11	+

The scheme listed in the PDG meson summary tables takes the $\omega(1420)$ as a $^3S_1$ state and $\omega(1650)$ as $^3D_1$. The ρ states run parallel, with $\rho(1450)$ as a $^3S_1$ state and the well-established $\rho_1(1700)$ as $^3D_1$. The $\phi(1680)$ fits in as $^3S_1$ and $\phi(1850)$ as $^3D_1$; the ϕ states lie higher than $n\bar{n}$ states by a similar mass difference to that between $f_2(1270)$ and $f_2(1525)$ (which is well established as $s\bar{s}$). Fitting the $\omega(1960)$ together with $\omega(1650)$ gives a slope of 1.091 ± 0.068, close to other CB slopes. Fitting the remaining $\omega(^3S_1)$ trajectory with states at 782, 1425, and 2205 MeV, but with two missing states, gives a slope of 1.080 ± 0.029. The fit to the second state, however, gives it a mass of 1329 MeV. Many authors have noticed this point. It could well be due to the fact that the ground state is abnormally low in mass, just as the J/ψ and $\Upsilon(1S)$ lie significantly below a straight line through $n = 2$, 3, and 4 radial excitations.

Section 3G of Ref. [1] considers f_0 states. Here physics remarks are required. One of the fundamentals of particle physics is chiral symmetry breaking. This was first proposed by Gell-Mann and Levy in 1960 [14]. It became well known to theorists that the attracive NN interaction requires the exchange of two correlated pions with a broad peak at 450–650 MeV, denoted by the σ. Bicudo and Ribiero provided a detailed account of how this arises [15]. The mechanism today accounts for the low mass $\sigma \equiv f_0(500)$, κ, $a_0(980)$ and $f_0(980)$. It is now well understood [16] how a crossover arises between these exceptional states and regular $q\bar{q}$ states near 1 GeV. The surviving mixing above 1 GeV is likely to push the $q\bar{q}$ 0^+ states up in mass. This can explain the anomalously high masses of $f_0(1370)$ and $a_0(1450)$. A further complication for f_0 is the likely existence of a glueball in the mass range 1500–1800 MeV, still obscure. A further point is that there is evidence [17] that the $f_2(1810)$ claimed by GAMS has been confused with the $f_0(1790)$ candidate for the radial excitation of $f_0(1370)$; the $f_0(1790)$ is consistent with the BES II 0^+ peak observed at 1812 MeV in $\omega\phi$ decays [18]. So, in summary, f_0 states are complex. Conclusions about the f_0 slope are, therefore, ambiguous. Using only the $\pi\pi$ mass of $f_0(1370)$ and the mass of $f_0(2330)$, the slope is 1.24 ± 0.045 GeV^2.

The $f_0(1370)$ decays dominantly to 4π; this introduces large dispersive effects on the mass. Crystal Barrel data at rest on $\bar{p}p \to 3\pi^0$ contain 600 000 precisely measured events, and interference effects between the three $\pi\pi$ components determine phase variations very precisely. The mass fitted to the $\pi\pi$ channel is $1309 \pm 1(\mathrm{stat}) \pm 15(\mathrm{syst})$ MeV. However, the rapidly increasing phase space for its dominant $\rho\rho$ decay channel moves the peak in 4π data up by $\sim$75 MeV. Pole positions on different sheets are given in Table 4 of Ref. [19] for $f_0(1370)$ and $f_0(1500)$ and are quite revealing. This strong threshold shifts the pole of $f_0(1370)$ by at most 17 MeV from the peak in $\pi\pi$; the fitted 2π full width is 325 MeV. So, in this extreme case, the shift in pole position is $\leq 10.5\%$ of the half-width. For the $f_0(1500)$, the shift in pole position is 8 MeV from the nominal mass compared with a half-width of 54.4 ± 3.5 MeV. These shifts are a factor at least 6 less than MAB assume.

MAB construct two trajectories for what they take to be $n\bar{n}$ states and $s\bar{s}$. The $n\bar{n}$ trajectory starts with $f_0(980)$ and finishes with $f_0(2200)$. However, there is almost universal agreement today that $f_0(980)$ and $a_0(980)$ are not $q\bar{q}$ states but have dominant 4-quark composition [20]. The $f_0(980)$ decays dominantly to $K\bar{K}$, not $\pi\pi$. BES II quote a $KK/\pi\pi$ branching ratio $4.21 \pm 0.2(\mathrm{stat}) \pm 0.21(\mathrm{syst})$ [21]; this is one of the very few experiments which has data on both $K\bar{K}$ and $\pi\pi$. A further important source of information is the decay of $\chi^0 \to K^+K^-$. There is a conspicuous $f_0(1710)$ in the data and a further peak at $f_0(2200)$ [22]. This suggests that they both have substantial $s\bar{s}$ components. So the MAB $n\bar{n}$ trajectory looks unlikely.

On their $s\bar{s}$ trajectory, MAB start with $f_0(1370)$ and finish with $f_0(2330)$. The $f_0(1370)$ is observed dominantly in decays to 4π, largely $\rho\rho$. It has a branching ratio to $K\bar{K}$ of 0.12 ± 0.06 in the CB data, so it does not look like an $s\bar{s}$ state. The last member of this trajectory is $f_0(2330)$. This has been observed in Crystal Barrel data in decays to $\pi\pi$ and $\eta\eta$ [8] with a flavor angle of 15.1°, so it is certainly not a dominantly $s\bar{s}$ state.

Section 3E of MAB [1] discusses a_0, a_2, and a_4 states. This is again a complex story. They use the mass of $a_0(980)$, which is unwise in view of its association with chiral symmetry breaking. The $a_0(1450)$ is well determined [23], but the signal for $a_0(2025)$ is very weak. An additional a_0 is to be expected somewhere between these two, but there are no data adequate to detect it; finding spin-0 states is difficult. Assuming this state has been missed, the slope from $a_0(1450)$ and $a_0(2025)$ is 0.96 ± 0.08 GeV^2 but is probably affected by chiral symmetry breaking and is not used in the overall CB average for the slope. MAB make the opposite assumption that this is the first radial excitation of $a_0(1450)$ and hence find a slope of 1.42 ± 0.26.

Moving on to a_2 states, MAB consider as an upper trajectory ($^3F_2$) $a_2(2030)$ and $a_2(2255)$ and arrive at a similar slope to CB. For the $^3P_2$ trajectory, they take $a_2(1320)$, $a_2(1700)$, and $a_2(2175)$. This is to be compared with the well-established f_2 trajectory $f_2(1270)$, $f_2(1565)$, $f_2(1910)$, and $f_2(2240)$. They miss an a_2 state to be identified with the $a_2(1950)$ of Anisovich *et al.* [24]. They find a slope 1.39 ± 0.26 compared with the CB determination 1.00 ± 0.06.

There is agreement between CB and MAB for the a_4 slope. However, one comment is needed on the PDG determination of the mass. It is determined largely by the data of Uman *et al.* [25]. If one looks at their Fig. 6, the difference in χ^2 between a_2 and a_4 is small. They do not consider the possibility that both a_2 and a_4 are present; that would not be at all surprising. Therefore, the CB determination of the mass is preferred here.

Consider next the f_2 states. The problem here is that MAB do not discriminate between the $^3P_2$ states and $^3F_2$, which are well separated in CB data. MAB launch into four alternative scenarios, all of which have problems.

Their f_2^a trajectory is made from $f_2(1370)$, $f_2(1750)$, and $f_2(2150)$. The $f_2(2150)$ is not seen in CB data. It is observed only in decays to $K\bar{K}$ and $\eta\eta$. The $f_2(2010)$ of the PDG [3], observed by Etkin *et al.*, in $\bar{p}p \to \phi\phi$ actually peaks at 2150 MeV. The mass quoted by Etkin *et al.* [26] is the K-matrix mass and can differ from the T-matrix mass; the K-matrix formalism assumes that all decay channels are known, but that is unlikely. The obvious interpretation of the $f_2(2150)$ is the $s\bar{s}$ partner of $f_2(1910)$, i.e., a $^3P_2$ state. Etkin *et al.* also report an $f_2(2300)$ in the $\phi\phi$ S wave and $f_2(2340)$ in the $\phi\phi$ D wave. This is naturally to be interpreted as an $s\bar{s}$ $^3F_2$ state. The $f_2(1750)$ of Schegelsky *et al.* [27] is observed in $\gamma\gamma \to K\bar{K}$ and is interpreted by them as an $s\bar{s}$ state—the radial excitation of $f_2(1525)$, though rather low in mass.

The MAB f_2^b trajectory uses $f_2(1430)$. That entry in PDG tables has a straightforward interpretation. The $\omega\omega$ channel (and therefore $\rho\rho$) couples strongly to $f_2(1565)$. When analyzing data on Dalitz plots, it is necessary to continue the Flatté formula for $f_2(1565)$ below the $\omega\omega$ threshold, rather than just cutting it off. This is the way in which Crystal Barrel analyzes Dalitz plots. The result is a cusp in the $\pi\pi$ channel at 1430 MeV; see Fig. 7 of Adomeit *et al.* [28]. It is likely that the data listed by the PDG under $f_0(1430)$ were due to this phenomenon.

The f_2^c trajectory of MAB starts with $f_2(1525)$, which is a well-known $s\bar{s}$ state and is obviously invalid. Their f_2^d trajectory uses $f_2(1565)$, $f_2(2000)$, and $f_2(2295)$, hence mixing $^3P_2$ and $^3F_2$ states. This is also invalid.

They continue with three further trajectories, the first based on $f_2(1640)$ together with $f_2(2150)$. The $f_2(1640)$ has been explained by Baker *et al.* [10] as the $\omega\omega$ decay of $f_2(1565)$; the rapidly rising $\omega\omega$ phase space shifts the peak in $\omega\omega$ up to 1640 MeV [10]. The second is based on the questionable $f_2(1810)$ and $f_2(2220)$, which is a very narrow peak, 23 MeV wide, claimed in BES II data. If such a narrow state contributes to nonstrange $q\bar{q}$ states, it is a mystery why it is not observed very conspicuously in CB data. Their final trajectory is made of $f_2(2010)$ and $f_2(2340)$, which are observed in $\phi\phi$ and $K\bar{K}$ and finds a slope of 1.43 ± 0.83 GeV^2; they are obvious candidates for $s\bar{s}$ states.

Section 3D of MAB [1] concerns π and π_2 trajectories. These agree with CB. The $\pi(1800)$ is usually considered as a hybrid candidate; it has little effect on the fitted slope.

Section 3C of Ref. [1] discusses ρ_1 and ρ_3 states. Their slope for the latter is close to the CB value but with a much larger error from their χ^2 criterion. The physics situation concerning ρ_1 states is a mess, for physics reasons. The $\rho(1450)$ couples weakly to 2π, and there are large dispersive effects in the 4π channel, which have not yet been taken into account. The natural interpretation of it is the $^3S_1$ radial excitation of $\rho(770)$, but the large slope may arise simply from the fact that the ground state is abnormally low, like the J/ψ and $\Upsilon(1S)$. The $\rho(1570)$ of *BABAR* has a larger error in mass: $\pm 36(\text{stat}) \pm 62(\text{syst})$ MeV and is marginally consistent with $\rho(1450)$, which actually has a mass of 1465 ± 25 MeV.

The $\rho(1900)$ can be identified with a recent Novosibirsk observation of a 6π peak almost exactly at the $\bar{p}p$ threshold [11]. This is likely to be a $^3S_1$ state captured by the very strong $\bar{p}p$ *S*-wave, but could be a nonresonant cusp.

CB data list ratios r_J of coupling constants to orbital angular momentum $L = J + 1$ and $L = J - 1$. The $\rho(2000)$ has a sizable r value 0.70 ± 0.23 requiring at least some $^3D_1$ contribution. The $\rho(2150)$ in CB data has an r value -0.05 ± 0.42, consistent with $^3S_1$. The $\rho(2270)$ in CB data has $r = -0.55 \pm 0.66$, which is ambiguous. However, the $\rho(2000)$, (2150), (2270) make a natural sequence of $^3D_1$, $^3S_1$, $^3D_1$. If this solution to the puzzle is accepted, the slope of the CB $^3S_1$ trajectory is 1.34 ± 0.03, with a rather poor fit to the mass of $\rho(1450)$. In view of the problems with $\rho(1450)$, this is not included in the grand average. The trajectory of $\rho(1700)$, $\rho(2000)$, and $\rho(2270)$ gives a slope of 1.17 ± 0.03; MAB quote 1.08 ± 0.47.

Section 3B of MAB [1] discusses η and η_2 states. The $\eta(548)$ is believed to be a Goldstone boson and should not be included in the assessement of $q\bar{q}$ states. The $\eta(1760)$ and $\eta(2100)$ were claimed by DM2 but later identified in Mark III data [29] as having $J^{PC} = 0^{++}$, although they sit on a large noninterfering 0^{-+} background [0^{++} and 0^{-+} do not interfere in J/ψ radiative decays after summing over relevant spin states of the J/ψ]. They are also identified in E760 data [30] in the $\eta\eta$ channel, where $J^{PC} = 0^{-+}$ is forbidden by Bose statistics. The remaining trajectory, $\eta(1295)$ and $\eta(2320)$, gives a CB slope of 1.24 ± 0.03; MAB quote 1.33 ± 0.11.

For η_2 states, the averaged slope agrees with the global average within errors, but the χ^2 of the fit to the $\eta_2(2030)$ in the middle is high. There is a likely explanation. There is an extra state $\eta_2(1870)$ which is naturally explained as a hybrid partner to $\pi_1(1600)$ predicted near this mass. By the usual level repulsion, this pushes the $\eta_2(1645)$ down and the $\eta_2(2030)$ up, although the overall effect on the average slope is small.

Section 3A of MAB [1] discusses the a_1 trajectory. The $a_1(2095)$ has a large error in the mass of ± 121 MeV. The $a_1(2270)$ completes the trajectory. There is an obvious problem that the $a_1(1260)$ has a large width; the PDG quotes it as 250–660 MeV. A recent *BABAR* estimate is $410 \pm 31 \pm 30$ MeV. The CB slope is 1.08 ± 0.06 GeV^2; MAB find 1.43 ± 0.26 GeV^2.

Finally, MAB discard all slope determinations which have only two points. This removes all the determinations from $^3F_2$, $^3F_3$, and $^3F_4$ states which are among the best. As one sees from Table I and Fig. 1, these determinations have slopes consistent with other CB values. MAB also assign $a_2(2030)$ and $a_2(2255)$ the radial quantum numbers $n = 2$ and 3, while the nearby $f_2(2000)$ and $f_4(2295)$ obviously have $n = 3$ and 4.

In summary, the MAB classification of slopes unfortunately contains a number of problems, and there is no significant case for the large slopes they claim for some cases.

V. EPILOGUE

Values of CB and MAB differ significantly only where there are clear problems in their selection of states in the fit. The weighted mean of CB slopes is revised slightly. On close inspection, the χ^2 contributions from $3S_1\rho_1$ results are high by a factor of 4. Warnings about the problem in this case have already been given. Likewise, contributions to χ^2 from a_0 are high by a factor of 5. Again the text has pointed out problems for these states. Finally, χ^2 contributions from a_2 $^3P_2$ states are high by a factor of 4. This is no surprise, since there are no polarization data to provide clear identifications of these states.

MAB remark that Anisovich, Anisovich, and Sarantsev proposed a scheme in the year 2000 in which the lowest $J^{PC} = 0^{++}$ states were taken as $a_0(980)$ and $f_0(980)$ [31]. Since then, there have been many studies of the effects of chiral symmetry breaking. It is now widely believed that the σ, κ, $a_0(980)$ and $f_0(980)$ are meson-meson states and that there is a crossover to $q\bar{q}$ states near 1 GeV, where chiral symmetry breaking decreases rapidly.

Summarizing, the mean slope without any corrections is 1.130 ± 0.011. Reducing the weights of the three troublesome cases to 1 modifies this to the final value 1.135 ± 0.012, compared with the old value of 1.143 ± 0.013 GeV^2. There is no clear case for the large error assessment of MAB. In fact, states with large widths already enlarge the errors for masses appropriately.

A comment on the MAB approach is that they adopt their assumption that meson masses can move by $\Gamma/2$ from theoretical predictions; those are that for large-N_c the strong coupling constant scales as $g \sim 1/\sqrt{N_c}$ with the result that meson masses change by $\Gamma/2$ when evolved from $N_c = 3$ to $N_c = \infty$; see the Refs. [16–18] given in their paper. The conclusion from the present analysis is that the N_c world is different from $N_c \rightarrow \infty$.

The PDG lists CB data under "other light mesons, further states: on the grounds that they need confirmation. Perhaps, but $I = 0$, $C = +1$ does contains a complete spectrum of expected states. For other isospin and C values, it is desirable to improve the database. That cannot be done in production experiments because the exchanged meson is not usually known, i.e., no polarization information is available. The ρ and ω states can be improved at VEPP 2 in Novosibirsk by using transversely polarized electrons. Two measurements are readily made of asymmetries normal to the plane of polarization and in the plane of polarization. Electron polarization of 70% is already achieved, and two detectors, CMD and SMD, are available and running. The presence of $^3D_1$ states is then revealed by distinctive azimuthal angular dependence in the polarization and can measure whether these are pure $^3D_1$ states or linear combinations with $^3S_1$, and if so how big the contributions are. Longitudinal polarization does not help much because it depends only on the difference of intensities of the two helicities available.

In order to trace the missing states above 1910 MeV, polarization measurements are needed for $I = 1$ $C = +1$ ($\eta\eta\pi^0$, $\eta\pi^0$ and $3\pi^0$), $I = 1$, $C = -1$ ($\omega\pi^0$ and $\eta\omega\pi^0$), and $I = 0$, $C = -1$ ($\omega\eta$ and $\omega\pi^0\pi^0$). Polarization data also introduce interference between singlet and triplet states, hence determining the singlet states much better. Data are required down to $\bar{p}$ momenta of ~360 MeV/c, the lowest momentum reached in the PS172 experiment [5]. The PANDA experiment cannot do this measurement because their lowest available beam momentum will be 1.5 GeV/c.

[1] P. Masjuan, E. R. Arriola, and W. Broniowski, Phys. Rev. D **85**, 094006 (2012).
[2] P. Masjuan, E. R. Arriola, and W. Broniowski, arXiv:1208.4472.
[3] J. Beringer *et al.*, Phys. Rev. D **86**, 010001 (2012).
[4] D. V. Bugg, Phys. Rep. **397**, 257 (2004).
[5] A. Hasan *et al.*, Nucl. Phys. **B378**, 3 (1992).
[6] E. Eisenhandler *et al.*, Nucl. Phys. **B96**, 109 (1975).
[7] C. Amsler *et al.* (Crystal Barrel Collaboration), Eur. Phys. J. C **23**, 29 (2002).
[8] A. V. Anisovich *et al.*, Phys. Lett. B **471**, 271 (1999).
[9] D. V. Bugg, J. Phys. G **35**, 075005 (2008).
[10] C. A. Baker *et al.*, Phys. Lett. B **467**, 147 (1999).
[11] E. P. Solodov, arXiv:1108.6174.
[12] F. Llanes-Estrada, S. Cotanch, I. General, P. Wang, G. Rupp, E. van Beveren, P. Bicudo, B. Hiller, and F. Kleefeld, AIP Conf. Proc. **1030**, 171 (2008).
[13] R. S. Longacre, Phys. Rev. D **42**, 874 (1990).
[14] M. Gell-Mann and M. Lévy, Nuovo Cimento **16**, 705 (1960).
[15] P. J. A. Bicudo and J. E. F. T. Ribiero, Phys. Rev. D **42**, 1611 (1990).
[16] W. Weise, Nucl. Phys. B, Proc. Suppl. **195**, 267 (2009).
[17] A. V. Anisovich, D. V. Bugg, V. A. Nikonov, A. V. Sarantsev, and V. V. Sarantsev, Phys. Rev. D **85**, 014001 (2012).
[18] M. Ablikim *et al.* (BES II Collaboration), Phys. Rev. Lett. **96**, 162002 (2006).
[19] D. V. Bugg, Eur. Phys. J. C **52**, 55 (2007).
[20] N. N. Achasov and G. N. Shestakov, Phys. Rev. D **81**, 094029 (2010).
[21] M. Ablikim *et al.* (BES II Collaboration), Phys. Lett. B **607**, 243 (2005).
[22] M. Ablikim *et al.* (BES II Collaboration), Phys. Rev. D **72**, 092002 (2005).
[23] D. V. Bugg, Phys. Rev. D **78**, 074023 (2008).
[24] A. V. Anisovich, C. A. Baker, C. J. Batty, D. V. Bugg, V. A. Nikonov, A. V. Sarantsev, V. V. Sarantsev, and B. S. Zou, Phys. Lett. B **517**, 261 (2001).
[25] I. Uman, D. Joffe, Z. Metreveli, K. Seth, A. Tomaradze, and P. Zweber, Phys. Rev. D **73**, 052009 (2006).
[26] A. Etkin *et al.*, Phys. Lett. B **201**, 568 (1988).
[27] V. A. Schegelsky, A. V. Sarantsev, V. A. Nikonov, and A. V. Anisovich Eur. Phys. J. A **27**, 207 (2006).
[28] J. Adomeit *et al.* (Crystal Barrel Collaboration) Nucl. Phys. **A609**, 562 (1996).
[29] D. V. Bugg, I. Scott, B. S. Zou, V. V. Anisovich, A. V. Sarantsev, T. H. Burnett, and S. Sutlief, Phys. Lett. B **353**, 378 (1995).
[30] T. A. Armstrong *et al.*, Phys. Lett. B **307**, 394 (1993).
[31] A. V. Anisovich, V. V. Anisovich, and A. V. Sarantsev, Phys. Rev. D **62**, 051502 (2000).